

Supporting Information

Computational insight into effective decomposition of NO_x gas pollutants using N-vacancies in graphitic carbon nitride

Yuewen Yang¹, Yanling Zhao^{1*}, Ruiqin Zhang^{1,2*}

¹ Department of Physics, City University of Hong Kong, Hong Kong SAR 999077, China

² Shenzhen JL Computational Science and Applied Research Institute, Shenzhen 518131, China

*Corresponding authors:

Prof. Rui-Qin Zhang (aprqz@cityu.edu.hk), Dr. Yanling Zhao (apzyl@cityu.edu.hk)

Authors

Rui-Qin Zhang – Department of Physics, City University of Hong Kong, Hong Kong SAR 999077, China; Shenzhen JL Computational Science and Applied Research Institute, Shenzhen 518131, China; orcid.org/0000-0001-6897-4010. E-mail: aprqz@cityu.edu.hk.

Yanling Zhao – Department of Physics, City University of Hong Kong, Hong Kong SAR 999077, China; orcid.org/0000-0001-5840-9149. E-mail: apzyl@cityu.edu.hk.

Yuewen Yang – Department of Physics, City University of Hong Kong, Hong Kong SAR 999077, China; orcid.org/0000-0003-0914-5276.

Table S1. Summary of current methods for NO_x removal.

No.	Methods	Advantages	Disadvantages				
1	Selective catalytic reduction (SCR) ^{S1} <table border="1" style="margin-left: 20px;"> <tr> <td>NH₃-SCR^{S2}</td> </tr> <tr> <td>H₂-SCR^{S3}</td> </tr> <tr> <td>HC-SCR^{S4}</td> </tr> <tr> <td>CO-SCR^{S5}</td> </tr> </table>	NH ₃ -SCR ^{S2}	H ₂ -SCR ^{S3}	HC-SCR ^{S4}	CO-SCR ^{S5}	High efficiency (>90%)	High cost, the complex system at high operation temperature (e.g., 400 °C for MnO _x ^{S6})
NH ₃ -SCR ^{S2}							
H ₂ -SCR ^{S3}							
HC-SCR ^{S4}							
CO-SCR ^{S5}							
2	Selective non-catalytic reduction (SNCR) ^{S7}	Catalyst-free, non-toxic products (e.g., H ₂ O and N ₂)	High temperature (850-1100°C)				
3	Wet scrubbing method ^{S8}	Catalyst-free	Product liquid waste and need large multi-stage scrubbers				
4	Electron beam ^{S9}	High ratio NO _x reduction (about 95% ^{S10})	Complexity of equipment structure, and shielding and preventing problems of radiation				
5	Adsorption methods ^{S11}	Cheap adsorbents (e.g., Zeolites ^{S11})	Huge amount of water and complex facilities				
6	Electrochemical method ^{S12}	Cost-effective, selective NO _x conversion of more than 70%	Producing NO ₃ ⁻				
7	Non-thermal plasma ^{S13}	Simultaneous treatment of pollutants, rapid start and stop, low capital and operation costs, good scalability, and integration with existing systems	The reactor's structure parameters significantly affect the characteristics of non-thermal plasma and pollutant removal efficiency.				

- [S1] Y. Sun, E. Zwolińska and A. G. Chmielewski, Abatement technologies for high concentrations of NO_x and SO₂ removal from exhaust gases: a review, *Critical Reviews in Environmental Science and Technology* **2016**, 46 (2): 119-142.
- [S2] F. Gao, X. Tang, H. Yi, S. Zhao, C. Li, J. Li, *et al.*, A review on selective catalytic reduction of NO_x by NH₃ over Mn-based catalysts at low temperatures: catalysts, mechanisms, kinetics and DFT calculations, *Catalysts* **2017**, 7, 7.
- [S3] Z. Hu and R. T. Yang, 110th anniversary: recent progress and future challenges in selective catalytic reduction of NO by H₂ in the presence of O₂, *Industrial & Engineering Chemistry Research* **2019**, 58 (24): 10140-10153.
- [S4] F. Gunnarsson, J. A. Pihl, T. J. Toops, M. Skoglundh and H. Härelind, Lean NO_x reduction over Ag/alumina catalysts via ethanol-SCR using ethanol/gasoline blends, *Applied Catalysis B: Environmental* **2017**, 202, 42-50.
- [S5] T. Liu, J. Qian, Y. Yao, Z. Shi, L. Han, C. Liang, *et al.*, Research on SCR of NO with CO over the Cu_{0.1}La_{0.1}Ce_{0.8}O mixed-oxide catalysts: effect of the grinding, *Molecular Catalysis* **2017**, 43, 43-53.
- [S6] C. Liu, F. Li, J. Wu, X. Hou, W. Huang, Y. Zhang, *et al.*, A comparative study of MO_x (M = Mn, Co, and Cu) modifications over CePO₄ catalysts for selective catalytic reduction of NO with NH₃, *Journal of Hazardous Materials* **2019**, 363, 439-446.
- [S7] M. Pronobis, R. Wejkowski, K. Jagodzińska and T. Kress, Simplified method for calculating SNCR system efficiency, *E3S Web of Conferences 2017 EDP Sciences* Pages: 02003.
- [S8] B. R. Deshwal, S. H. Lee, J. H. Jung, B. H. Shon and H. K. Lee, Study on the removal of NO_x from simulated flue gas using acidic NaClO₂ solution, *Journal of Environmental Sciences* **2008**, 20 (1): 33-38.
- [S9] A. Basfar, O. Fageeha, N. Kunnummal, A. Chmielewski, J. Licki, A. Pawelec, *et al.*, A review on electron beam flue gas treatment (EBFGT) as a multicomponent air pollution control technology, *Nukleonika* **2010**, 55, 271-277.
- [S10] J. Licki, A. G. Chmielewski, A. Pawelec, Z. Zimek and S. Witman, Electron beam treatment of exhaust gas with high NO_x concentration, *Physica Scripta* **2014**, T161, 014067.
- [S11] F. Rezaei, A. A. Rownaghi, S. Monjezi, R. P. Lively and C. W. Jones, SO_x/NO_x removal from flue gas streams by solid adsorbents: a review of current challenges and future directions, *Energy & Fuels* **2015**, 29 (9): 5467-5486.
- [S12] J. Shao, Y. Tao and K. K. Hansen, Highly selective NO_x reduction for diesel engine exhaust via an electrochemical system, *Electrochemistry Communications* **2016**, 72, 36-40.
- [S13] P. Talebizadeh, M. Babaie, R. Brown, H. Rahimzadeh, Z. Ristovski and M. Arai, The role of non-thermal plasma technique in NO_x treatment: A review, *Renewable and Sustainable Energy Reviews* **2014**, 40, 886-901.

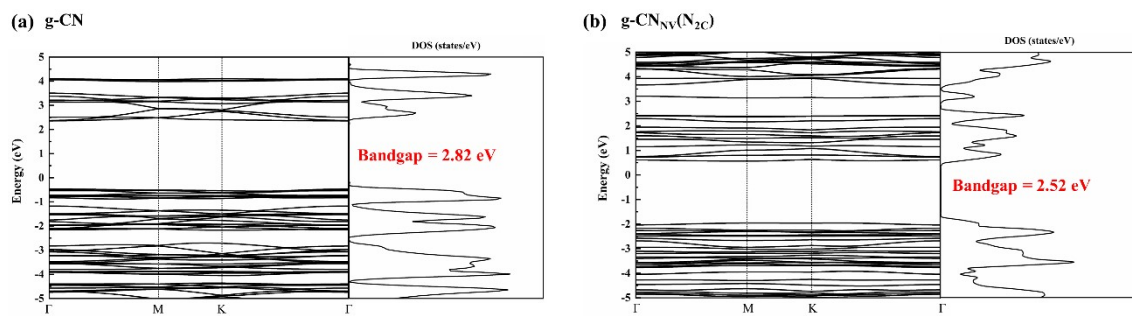


Figure S1. The band structure and density of states for **(a)** pristine g-CN and **(b)** g-CN_{NV} (N₂C) calculated by HSE06 hybrid functional.

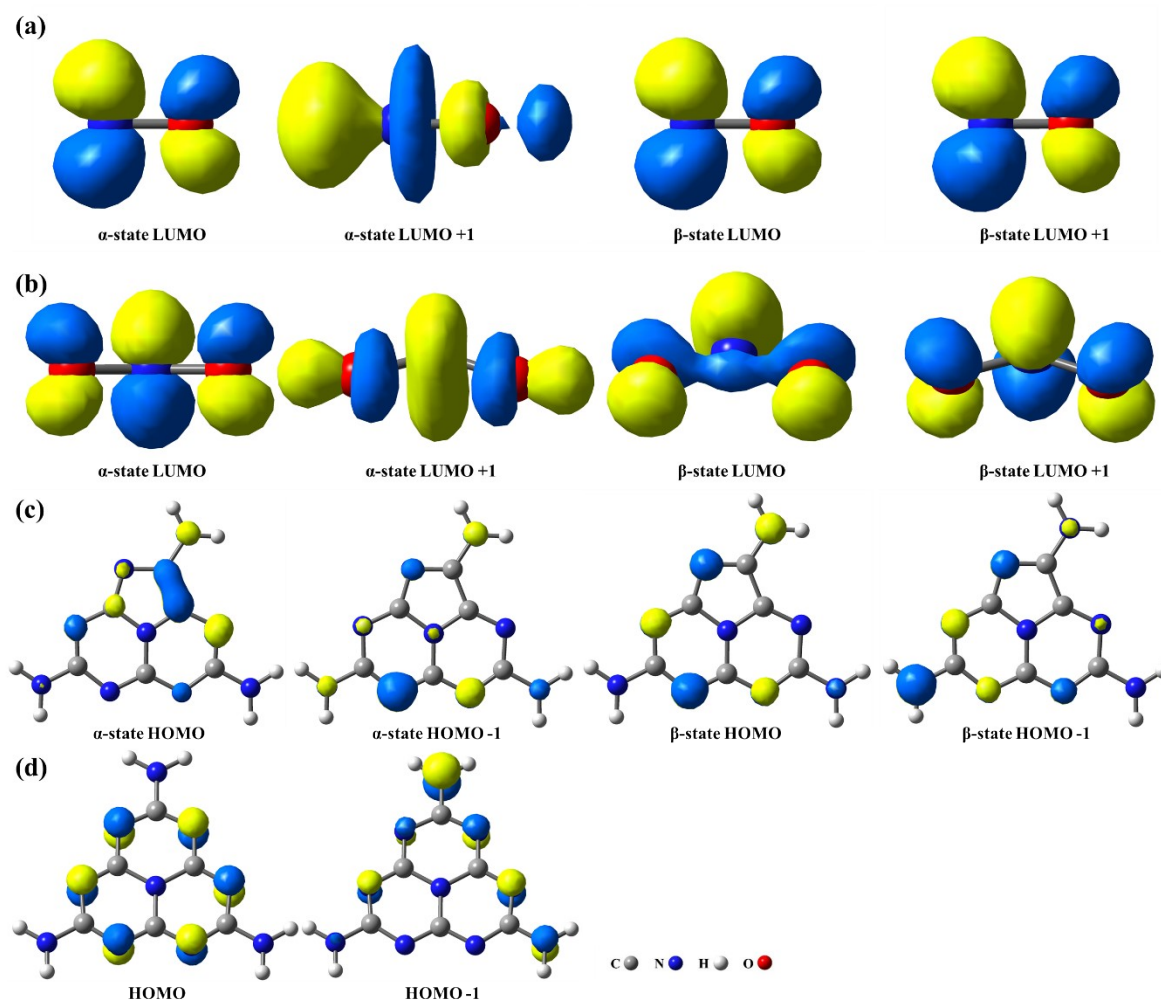


Figure S2. Frontier molecular orbitals (MO) of NO, NO₂, Heptazine_{NV}, and Heptazine clusters before their gas-solid interactions: **(a)** lowest unoccupied MO (LUMO) and nearby LUMO+1 in α and β states for NO; **(b)** LUMO and LUMO+1 in α and β states for NO₂; **(c)** highest occupied MO (HOMO) and nearby HOMO-1 in α and β states for Heptazine_{NV} with N_{2C}; **(d)** HOMO and HOMO-1 for Heptazine. The isovalues of all MOs are set as 0.08 a.u. to give a clear illustration.

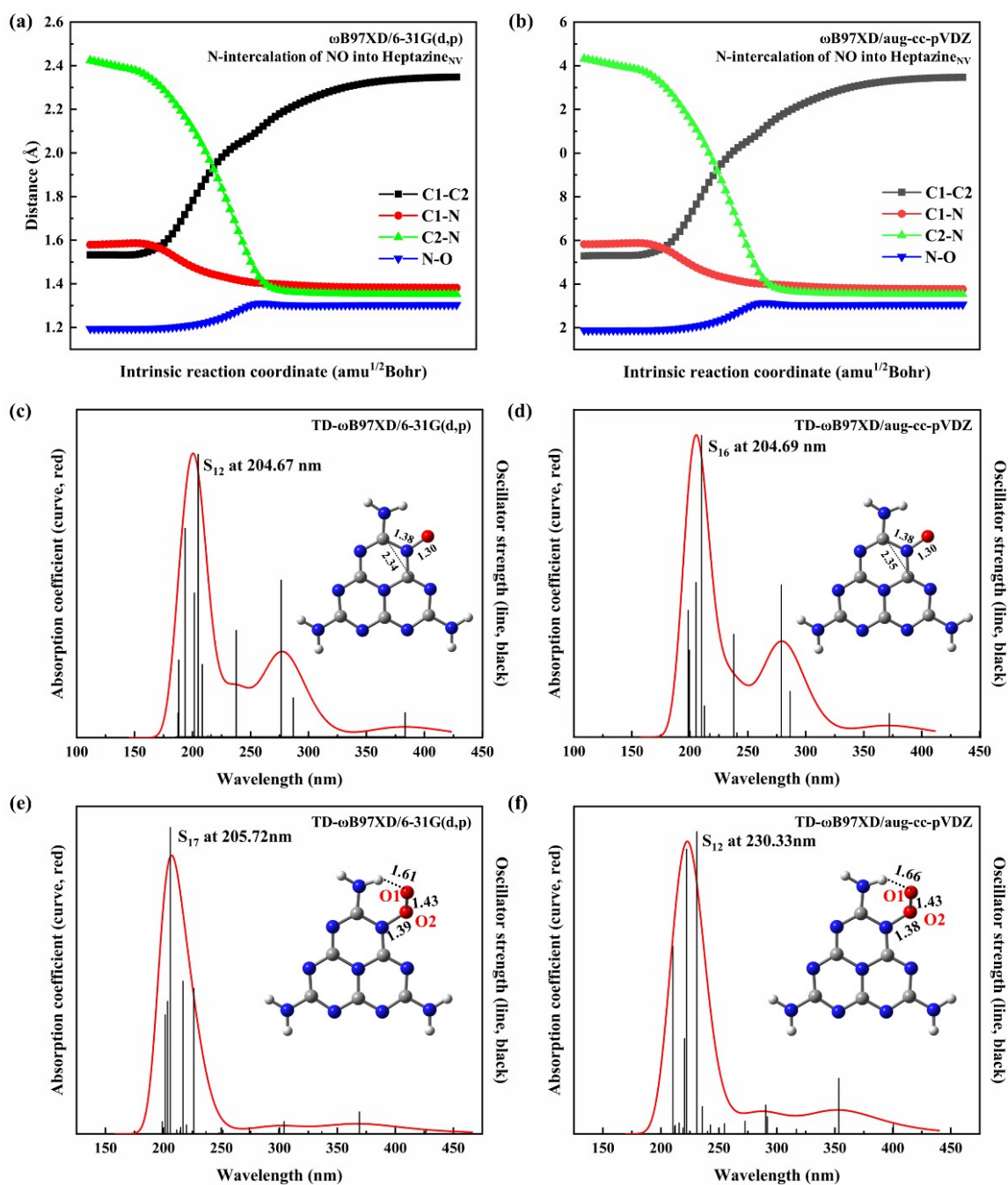


Figure S3. Key interatomic distance evolutions of D_{C1-C2} , D_{C1-N} , D_{C2-N} , and D_{N-O} during the N-intercalation of NO into Heptazine_{NV} in the ground state (S_0) by (a) ω B97XD/6-31G(d,p) and (b) ω B97XD/aug-cc-pVDZ. UV-vis absorption spectra of O@Heptazine calculated by (c) TD- ω B97XD/6-31G(d,p) and (d) TD- ω B97XD/aug-cc-pVDZ, with the significant light-absorption peaks of S_{12} at 204.72 nm and S_{16} at 204.69 nm marked. UV-vis absorption spectra of ¹O₂@Heptazine calculated by (e) TD- ω B97XD/6-31G(d,p) and (f) TD- ω B97XD/aug-cc-pVDZ, with the significant light-absorption peaks of S_{17} at 205.72 nm and S_{12} at 230.33 nm marked.

Table S2. The energy data (Unit: eV) for the oxygen release from Heptazine as the function of D_{N-O_2} during the NO decomposition.

D_{N-O_2}	E (S ₀ , relaxed scan)	E (S ₁ , rigid scan)	E (T ₁ , rigid scan)	E (T ₀ , rigid scan)	E (T ₀ , relaxed scan)	E (S ₀ , relaxed scan)	E (S ₁ , rigid scan)	E (T ₁ , rigid scan)	E (T ₀ , rigid scan)	E (T ₀ , relaxed scan)
	by ω B97XD/6-31G(d,p)					by ω B97XD/aug-cc-pVDZ				
1.38	-3.24	-0.32	0.04	-0.36	-1.79	-3.11	-0.01	0.19	-0.21	1.46
1.4	-3.24	-0.33	0.03	-0.36	-1.83	-3.11	-0.02	0.19	-0.26	-1.58
1.5	-3.18	-0.25	-0.34	-0.36	-2.18	-3.02	0.07	-0.07	-0.19	-1.93
1.6	-3.17	-0.95	-1.77	-0.48	-2.64	-2.97	-0.70	-1.47	-0.08	-2.39
1.7	-3.25				-3.19	-3.02				-2.93
1.8	-3.38				-3.72	-3.13				-3.46
1.9	-3.52				-4.17	-3.25				-3.91
2.0	-3.63				-4.53	-3.36				-4.28
2.1	-3.71				-4.81	-3.45				-4.55
2.2	-3.77				-5.02	-3.51				-4.76
2.3	-3.81				-5.16	-3.58				-4.91
2.4	-3.83				-5.27	-3.62				-5.02
2.5	-3.84				-5.34	-3.64				-5.09
2.6	-3.85				-5.39	-3.65				-5.15
2.7	-3.85				-5.42	-3.65				-5.19
2.8	-3.85				-5.44	-3.65				-5.21
2.9	-3.85				-5.46	-3.65				-5.23
3.0	-3.85				-5.48	-3.65				-5.25

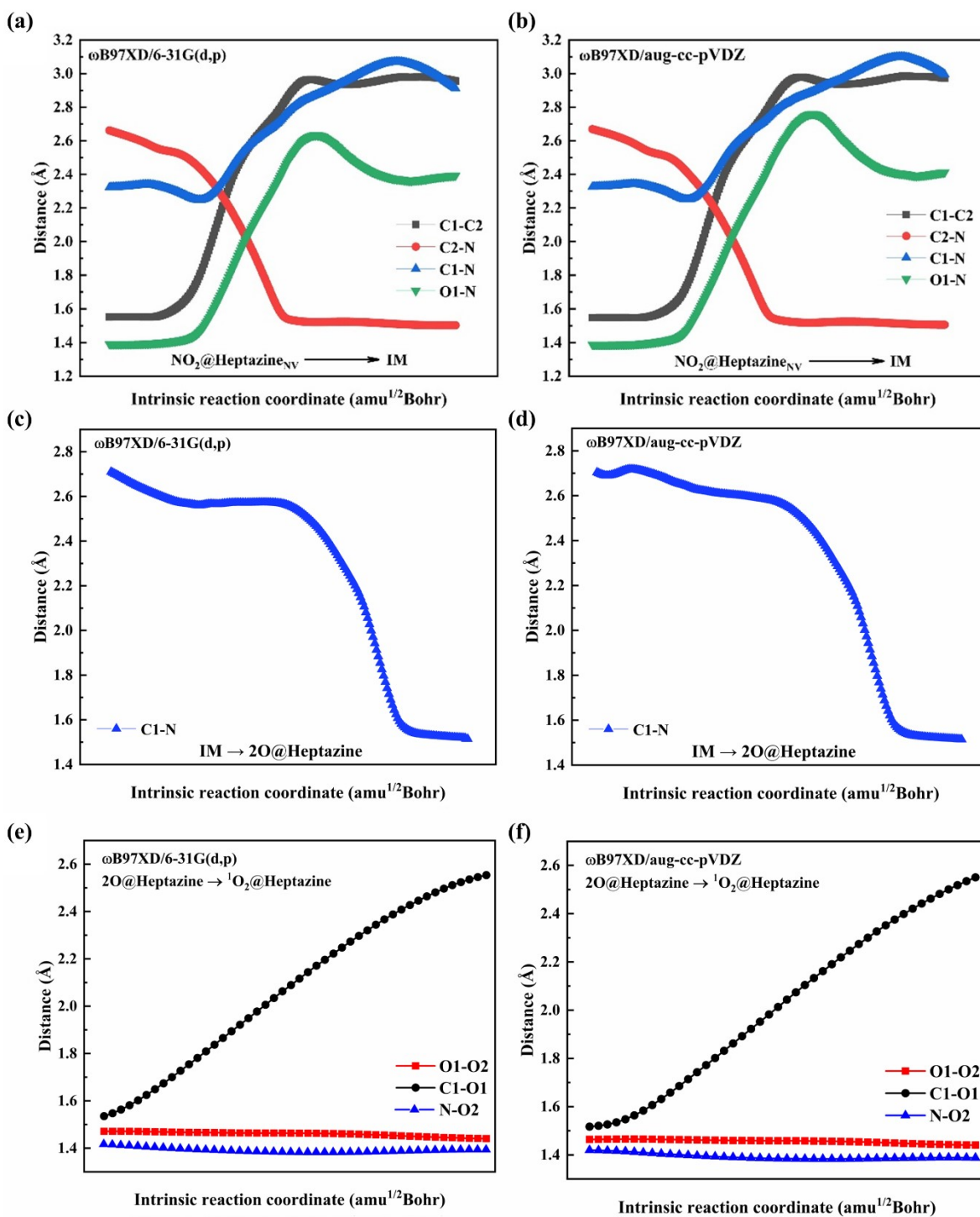


Figure S4. (a-d) Key interatomic distance evolutions of $D_{\text{C1-C2}}$, $D_{\text{C1-N}}$, $D_{\text{C2-N}}$, and $D_{\text{O1-N}}$ during the N-intercalation of NO_2 into $\text{Heptazine}_{\text{NV}}$ by IRC calculations of ω B97XD/6-31G(d,p) and ω B97XD/aug-cc-pVDZ in the ground state (S_0). (e, f) Key interatomic distance evolutions of $D_{\text{C1-O1}}$, $D_{\text{N-O2}}$, and $D_{\text{O1-O2}}$ during the ${}^1\text{O}_2$ formation on Heptazine by IRC calculations of ω B97XD/6-31G(d,p) and ω B97XD/aug-cc-pVDZ in S_0 .

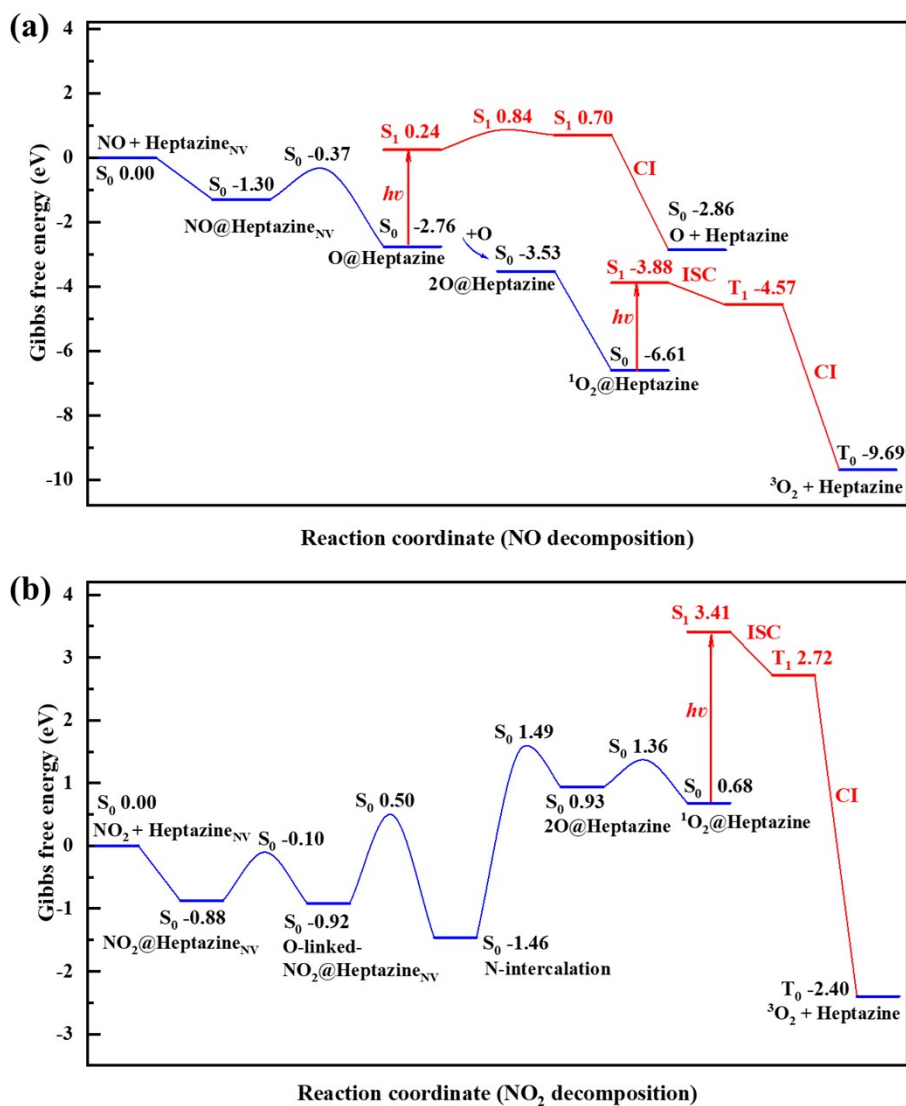


Figure S5. Gibbs free energy profiles of (a) NO and (b) NO₂ decompositions on Heptazine_{NV} at $T = 500$ K and $P = 1.00$ atm by ω B97XD/6-31G(d,p) calculations. The free energy values relative to the initial reactants of NO/NO₂ and Heptazine_{NV} are labelled to indicate the barrier (G_b) and change (ΔG) for each step.

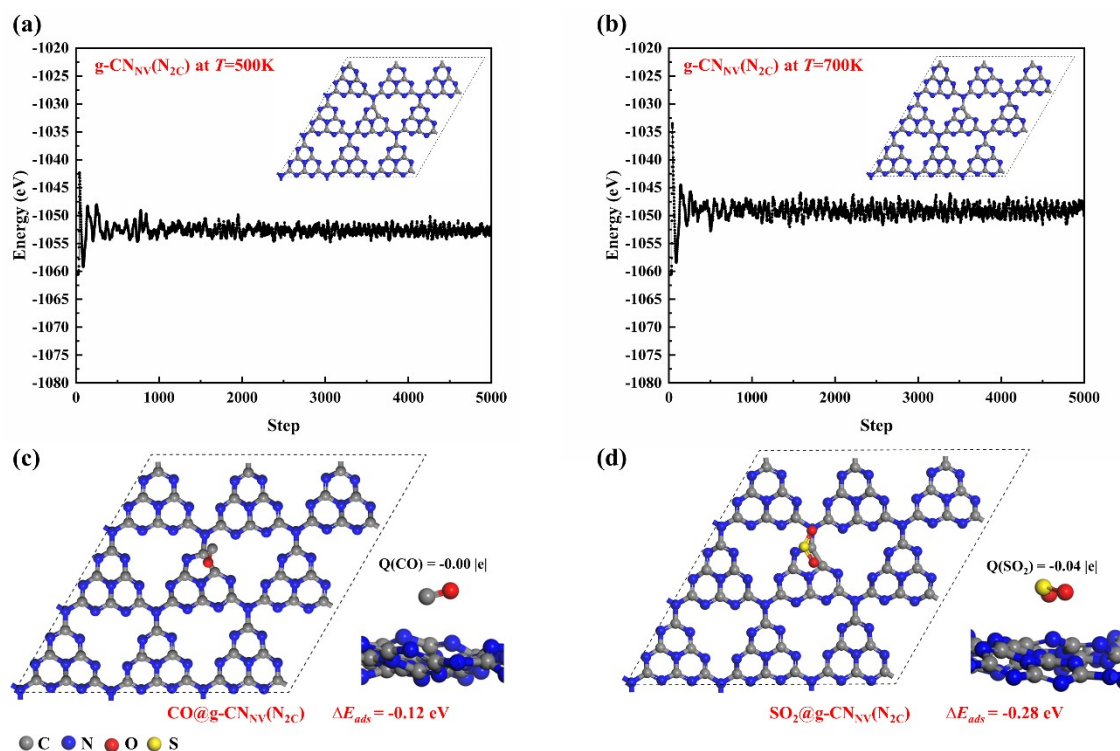


Figure S6. The total energy changes of g-CN_{NV} (N₂C) during AIMD simulations of 10ps with a time step of 2fs at (a) $T = 500\text{K}$ and (b) $T = 700\text{K}$, with the final configurations of g-CN_{NV} (N₂C) at 10ps inserted. Top views and side views (bottom right) of adsorption configurations of (c) CO and (d) SO₂ on g-CN_{NV} (N₂C) by GGA/PBE optimizations, with the charges (Q) on CO/SO₂ and adsorption energies (ΔE_{ads}) marked.

Table S3. The Gibbs free energy changes (ΔG in eV) and free energy barriers (G_b in eV) for NO and NO₂ decompositions on Heptazine_{NV} at $T = 300$ K and 500 K under $P = 1.00$ atm by ω B97XD/6-31G(d,p) calculations.

Gas-solid reactions between NO/NO₂ and Heptazine_{NV}	$T = 300$ K		$T = 500$ K	
	G_b	ΔG	G_b	ΔG
NO decomposition				
NO+Heptazine _{NV} (S ₀) → NO@Heptazine _{NV} (S ₀)	—	-1.65	—	-1.30
NO@Heptazine _{NV} (S ₀) → O@Heptazine (S ₀)	0.92	-0.93	0.93	-1.43
O@Heptazine (S ₀) → O@Heptazine (S ₁)	—	2.95	—	3.00
O@Heptazine (S ₁) → O + Heptazine (S ₀)	0.66	-2.90	0.60	-3.10
O + O@Heptazine (S ₀) → 2O@Heptazine (S ₀)	—	-0.85	—	-0.77
2O@Heptazine (S ₀) → O ₂ @Heptazine (S ₀)	—	-3.13	—	-3.08
O ₂ @Heptazine (S ₀) → O ₂ @Heptazine (S ₁)	—	2.75	—	2.73
O ₂ @Heptazine (S ₁) → O ₂ @Heptazine (T ₁)	—	-0.74	—	-0.69
O ₂ @Heptazine (T ₁) → ³ O ₂ + Heptazine (T ₀)	—	-4.72	—	-5.12
NO₂ decomposition	G_b	ΔG	G_b	ΔG
NO ₂ +Heptazine _{NV} (S ₀) → NO ₂ @Heptazine _{NV} (S ₀)	—	-1.30	—	-0.88
NO ₂ @Heptazine _{NV} (S ₀) → O-linked-NO ₂ @Heptazine _{NV} (S ₀)	0.77	-0.03	0.98	-0.04
O-linked-NO ₂ @Heptazine _{NV} (S ₀) → N-intercalation (S ₀)	1.40	-0.52	1.42	-0.54
N-intercalation (S ₀) → 2O@Heptazine (S ₀)	2.89	2.32	2.95	2.39
2O@Heptazine (S ₀) → O ₂ @Heptazine (S ₀)	0.35	0.01	0.43	0.25
O ₂ @Heptazine (S ₀) → O ₂ @Heptazine (S ₁)	—	2.75	—	2.73
O ₂ @Heptazine (S ₁) → O ₂ @Heptazine (T ₁)	—	-0.74	—	-0.69
O ₂ @Heptazine (T ₁) → ³ O ₂ + Heptazine (T ₀)	—	-4.72	—	-5.12